Electronic Supplementary Information for

A Singlet Oxygen Photosensitizer Enables Photoluminescent Monitoring of Singlet Oxygen Doses

Youngmin You,[a]* Eun Jin Cho,[b] Hyeokseon Kwon,[a] Jieun Hwang,[a] and Seung Eun Lee[a]

[a]Division of Chemical Engineering and Materials Science, Ewha Womans University, Seoul 120-750, Korea.

[b]Department of Advanced Materials Engineering for Information and Electronics, Kyung Hee University, Gyeonggi-do 446-710, Korea.

Experimental Details

Materials and General Methods

Commercially available chemicals were used as received. Anhydrous CH_2Cl_2 was purchased from Aldrich, and used without further drying. Phosphate buffered saline (PBS) was purchased from Sigma. PBS buffer solutions (10 mM) were prepared in milli-Q grade water (18.2 MΩ·cm), and by adjusting the pH to 7.4 with standard KOH (45 wt %, Aldrich) and HCl (1 N, Fluka) solutions. EJ1 stock solution was dissolved in DMSO (Aldrich) to 10 mM and stored frozen. The solution was thawed before spectroscopic measurements. Typically, 30 μL of the EJ1 stock solution was delivered to 3.0 mL of the pH 7.4 PBS buffer solution containing 10 vol % DMSO. Therefore, the concentration of EJ1 in the mixture of PBS and DMSO was 10 μM. DMSO was emloyed to suppress particulate formation. A 1 cm × 1 cm fluorimeter cell with a Teflon stopper (Hellma) was used for optical measurements. All the steady-state photophysical measurements were performed at 37 °C, unless otherwise stated. Solutions of $O_2^{\bullet-}$, OCl^-, *t*-BuO• and •OH were prepared by adopting the previous methods.[1,2] *t*-BuOOH and H_2O_2 were purchased from Aldrich and used as received. Photoirradiation of O_2-bubbled solutions (PBS(pH 7.4):DMSO = 9:1, v/v) containing methylene blue (Sigma, 1 μM) or Irpbt–TEG (10 μM) was performed to generate $^1O_2$. ^1H and $^{13}C\{^1H\}$ NMR spectra were collected with Bruker Ultrashield 500, 400 and 300 plus NMR spectrometers, and a Jeol JNM-AL300 spectrometer. Chemical shifts were referenced to TMS. Electrospray ionization mass spectra were obtained by employing a Thermo Electrons Co. Finnigan LCQ Advantage Max spectrometer.

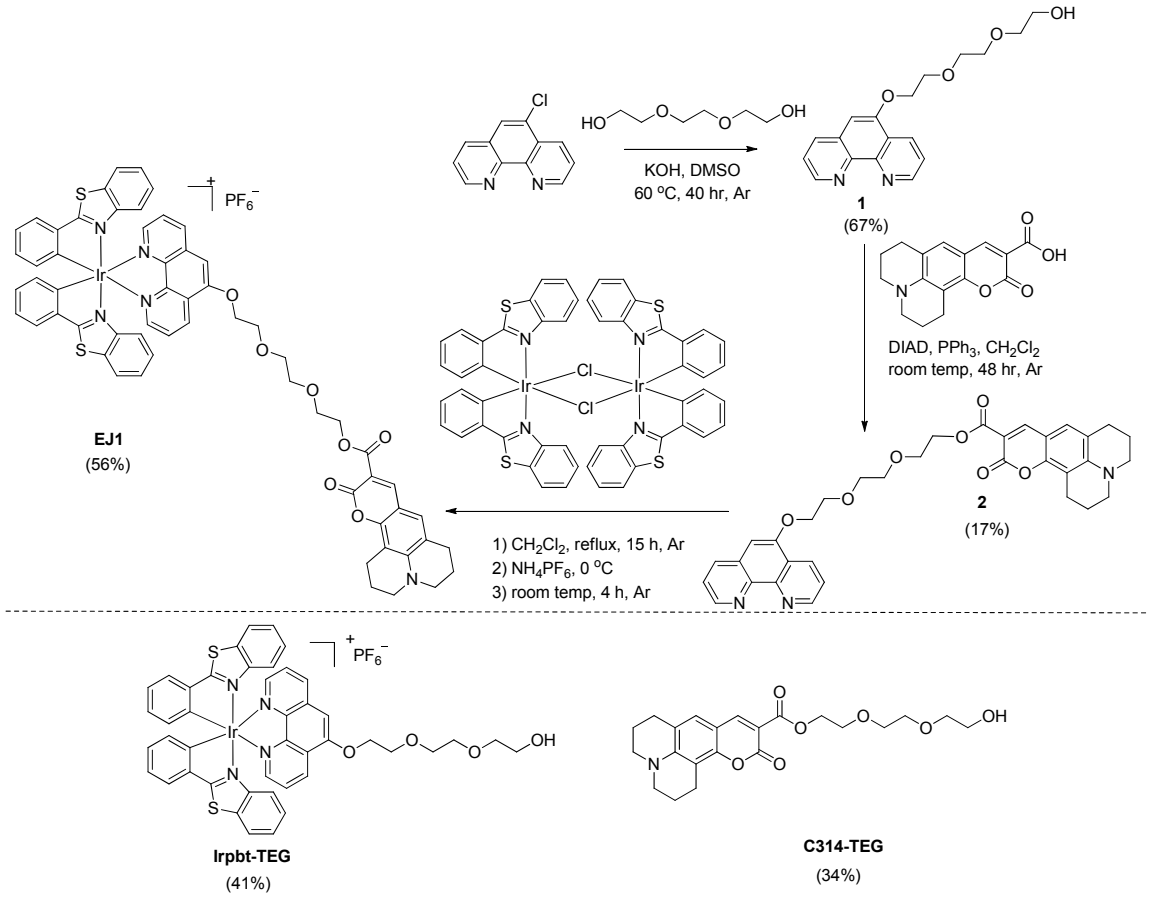

Scheme S1. Synthetic route to EJ1 and the chemical structures of Itpbt–TEG and C314–TEG

Synthesis of 1. To a stirred DMSO solution (100 mL) of triethylene glycol (9.79 g, 65.2 mmol), KOH (3.66 g, 65.2 mmol) was added. After 1 h at room temperature, 5-chloro-1,10-phenanthroline (2.80 g, 13.0 mmol) was delivered to the solution that was stirred for additional 40 h at 60 °C. The reaction mixture was poured onto 200 mL EtOAc, and washed thoroughly with water (300 mL × five times) to remove DMSO. The organic layer was recovered, dried over anhydrous $MgSO_4$, and concentrated under vacuum. Silica gel column purification was performed with increasing polarity of eluents from 100% CH_2Cl_2 to CH_2Cl_2:CH_3OH = 9:1 (v/v) to furnish yellow liquid in a 67% yield. ^{1}H NMR (400 MHz, $CDCl_3$) δ: 3.47 (m, 2H), 3.64 (m, 2H), 3.75 (m, 4H), 3.83 (m, 2H), 4.07 (t, J = 4.8 Hz, 2H), 4.44 (t, J = 4.8 Hz, 2H), 6.98 (s, 1H), 7.56 (dd, J = 8.2, 4.0 Hz, 1H), 7.65 (dd, J = 8.4, 4.4 Hz, 1H), 8.72 (d, J = 6.4 Hz, 1H), 9.0 (m, 1H), 9.2 (m, 1H). ^{13}C{^{1}H} NMR (100 MHz, $CDCl_3$) δ: 61.76, 68.06, 69.64, 70.53, 71.10, 72.64, 101.88, 122.72, 123.31, 123.65, 129.20, 131.09, 134.75,

142.98, 146.79, 148.01, 150.73, 152.16. MS (ESI, positive mode) *m*/*z* 329.20 ($[M+H]^+$). HR MS (FAB^+, *m*-NBA): Calcd for $C_{18}H_{21}N_2O_4$ ($[M+H]^+$), 329.1501; found, 329.1502.

Synthesis of 2. **1** (0.400 g, 1.21 mmol), coumarin 343 (0.379 g, 1.33 mmol), diisopropyl azodicarboxylate (0.368 g, 1.82 mmol), and triphenylphosphine (0.477 g, 1.82 mmol) were added into a 100 mL round-bottom flask. Anhydrous CH_2Cl_2 (70 mL) was delivered into the flask using a glass syringe under an Ar atmosphere. The reaction mixture was stirred for 48 h at room temperature, and then, concentrated under a reduced pressure. Silica gel column purification was performed using CH_2Cl_2:CH_3OH eluents with increasing the volume fraction of CH_3OH from 2 vol % to 10 vol %. Brown solid was obtained in a 17% yield. ^1H NMR (300 MHz, $CDCl_3$) δ: 1.87 (m, 4H), 2.58 (t, J = 6.3 Hz, 2H), 2.70 (t, J = 6.3 Hz, 2H), 3.22 (m, 4H), 3.83 (m, 4H), 3.88 (t, J = 5.2 Hz, 2H), 4.09 (t, J = 5.3 Hz, 2H), 4.38 (t, J = 4.4 Hz, 2H), 4.49 (t, J = 4.6 Hz, 2H), 6.71 (s, 1H), 6.91 (s, 1H), 7.53 (dd, J = 8.1, 4.6 Hz, 1H), 7.61 (dd, J = 8.3, 4.4 Hz, 2H), 8.08 (dd, J = 8.2, 1.7 Hz, 1H), 8.26 (s, 1H), 8.64 (dd, J = 8.3, 1.7 Hz, 1H), 9.00 (dd, J = 4.4, 1.9 Hz, 1H), 9.15 (dd, J = 4.3, 1.8 Hz, 1H). $^{13}C\{^1H\}$ NMR (125 MHz, $CDCl_3$) δ: 20.05, 21.02, 27.26, 29.71, 30.90, 41.02, 49.80, 50.21, 64.00, 68.22, 29.29, 29.64, 70.93, 101.76, 107.37, 119.16, 122.64, 123.17, 126.87, 128.52, 129.24, 131.06, 132.15, 134.74, 142.82, 146.57, 147.72, 148.57, 149.31, 150.64, 152.20, 153.35, 158.56, 164.40. HR MS (FAB^+, *m*-NBA): Calcd for $C_{34}H_{34}N_3O_7$ ($[M+H]^+$), 596.2347; found, 596.2401.

Synthesis of EJ1. The chloride-bridge dinuclear iridium precursor of 2-phenylbenzothiazole ($[(\mu\text{-Cl})Ir(pbt)_2]_2$, pbt = 2-phenylbenzothiazolate) was prepared following the procedure reported previously.[3] A 50 mL two-necked round-bottom flask was charged with **2** (47 mg, 80 μmol) and $[(\mu\text{-Cl})Ir(pbt)_2]_2$ (52 mg, 40 μmol). Anhydrous CH_2Cl_2 (30 mL) was added into the flask, and the reaction mixture was refluxed for 15 h under an Ar atmosphere. Then, NH_4PF_6 (130 mg, 800 μmol) was slowly added into the solution at 0 °C, and the solution was stirred for additional 4 h at room temperature. The reaction mixture was passed through a glass filter to remove the residual NH_4PF_6, and concentrated through vacuum. Flash column chromatography on silica gel and further purification employing preparative TLC techniques were performed to yield orange powder (56%). ^1H NMR (400 MHz, CD_3CN) δ: 1.78 (m, 4H), 2.53 (m, 4H), 3.25 (m, 4H), 3.64–3.71 (br m, 6H), 4.00 (m, 2H), 4.21–4.31 (br m, 2H), 4.38 (m, 2H), 5.82 (d, J = 8.4 Hz, 1H), 5.92 (d, J = 8.4 Hz, 2H), 6.48 (t, J = 7.6 Hz, 2H), 6.72 (s, 1H), 6.84–6.95 (br m, 4H), 7.15 (t, J = 7.2 Hz, 2H), 7.24 (td, J = 7.2, 0.8 Hz, 2H), 7.36 (s, 1H), 7.52 (m, 1H), 7.58–7.67 (br m, 1H), 7.76 (dd, J = 8.0, 4.8 Hz, 1H), 7.88 (dd, J = 8.4, 5.2 Hz, 1H), 7.94 (m, 4H), 8.14 (s, 1H), 8.25 (dd, J = 5.2, 1.2 Hz, 1H), 8.43 (dd, J = 8.4, 1.2 Hz, 1H), 8.46 (dd, J = 5.2, 1.2 Hz, 1H), 8.85 (dd, J = 8.4, 1.6 Hz, 1H). $^{13}C\{^1H\}$ NMR

(100 MHz, CD_3CN) δ: 20.61, 20.80, 21.79, 22.28, 27.98, 50.42, 50.91, 55.40, 64.77, 69.86, 69.90, 70.11, 70.67, 71.49, 71.61, 104.41, 106.08, 107.35, 108.06, 120.64, 126.97, 127.02, 127.10, 127.85, 128.01, 128.80, 129.12, 129.68, 129.80, 132.57, 132.63, 132.78, 132.95, 134.48, 135.06, 138.46, 141.69, 141.75, 144.83, 149.27, 149.78, 150.07, 150.20, 150.29, 150.79, 150.92, 153.05, 154.46, 154.75, 158.83, 165.04, 182.70. MS (ESI, positive mode) *m*/*z* 1208.07 ($[M–PF_6]^+$). HR MS (FAB^+, *m*-NBA): Calcd for $C_{60}H_{49}IrN_5O_7S_2$ ($[M–PF_6]^+$), 1208.2703; found, 1208.2698.

Synthesis of Irpbt–TEG. **Irpbt–TEG** was prepared employing the synthetic method identical to the procedure of **EJ1**, except using **1** instead of **2**. Brown powder (41%). ^1H NMR (300 MHz, $CDCl_3$) δ: 3.61 (m, 2H), 3.68–3.79 (br m, 7H), 4.06 (m, 2H), 4.58 (m, 2H), 5.83 (d, J = 2.7 Hz, 2H), 6.49 (t, J = 11 Hz, 2H), 6.93 (m, 5H), 7.14 (t, J = 10 Hz, 2H), 7.61 (s, 1H), 7.76–7.87 (br m, 7H), 8.17 (d, J = 5.1 Hz, 1H), 8.38 (dd, J = 7.1, 2.0 Hz, 1H), 8.72 (dd, J = 12, 2.0 Hz, 1H), 9.05 (dd, J = 11, 2.2 Hz, 1H). MS (ESI, positive mode) *m*/*z* 999.13 ($[M+NaCl]^+$).

Synthesis of C314–TEG. The synthetic method of the preparation of **2** was employed, except using triethylene glycol instead of **1**. White powder (34%). ^1H NMR (400 MHz, $CDCl_3$) δ: 1.98 (m, 4H), 2.76 (t, J = 6.5 Hz, 2H), 2.87 (t, J = 6.4 Hz, 2H), 3.33 (m, 3H), 3.58 (m, 2H), 3.64–3.69 (br m, 4H), 3.73 (m, 2H), 3.82 (m, 2H), 4.44 (m, 2H), 6.94 (s, 1H), 8.34 (s, 1H). $^{13}C\{^1H\}$ NMR (100 MHz, $CDCl_3$) δ: 15.39, 20.33, 21.43, 50.14, 50.15, 64.29, 66.86, 69.45, 70.07, 70.92, 106.76, 107.02, 107.76, 119.37, 127.24, 148.79, 149.52, 158.84, 164.41. MS (ESI, positive mode) *m*/*z* 440.16 ($[M+Na]^+$).

Steady-State UV–vis Absorption Measurements. UV–vis absorption spectra were collected on an Agilent Cary 300 spectrophotometer. 10 μM or 50 μM solutions were used for the measurements unless otherwise mentioned.

Steady-State Photoluminescence Measurements. Photoluminescence spectra were obtained using a Quanta Master 400 scanning spectrofluorimeter at 37 °C. The temperature was maintained by employing a water circulator. The 10 μM solutions were used for the measurements. Excitation wavelengths for EJ1, C314–TEG and Irpbt–TEG were 330 nm. The photoluminescence quantum yields (PLQYs) were relatively determined according to the following standard equation: $PLQY = PLQY_{ref} \times (I/I_{ref}) \times (A_{ref}/A) \times (n/n_{ref})^2$, where A, I, and n are the absorbance at the excitation wavelength, integrated photoluminescence intensity, and the refractive index of the solvent, respectively. 9,10-Diphenylanthracene in toluene solution was used as the external reference ($PLQY_{ref} = 1.00$).

Photoluminescence Lifetime Measurements. 50 μM solutions in Ar-saturated CH_3CN were used for determination of the photoluminescence lifetimes. Photoluminescence decay traces were

acquired based on time-correlated single-photon-counting (TCSPC) techniques using a FluoTime 200 instrument (PicoQuant, Germany) after pico- (λ_{obs} = 484 nm) and nanosecond (λ_{obs} = 600 nm) pulsed laser excitation. A 377 nm diode laser (PicoQuant, Germany) was used as the excitation source. The photoluminescence signals at 484 nm and 600 nm were obtained through an automated motorized monochromator. Photoluminescence decay profiles were analyzed using single (λ_{obs} = 600 nm) or double (λ_{obs} = 484 nm) exponential decay models embedded in an OriginLab, OriginPro 8.0 software.

Cell Culture. HeLa, A549, MCF7 and RAW 264.7 cells were grown in Dulbecco's modified Eagles's medium (DMEM with 4.5 g L^{-1} glucose, L-glutamate and sodium pyruvate; Corning) containing 10% fetal bovine serum (FBS) and 50 μg mL^{-1} penicillin at 37 ºC and 5% CO_2.

Visualization of Endogenously Produced $^1O_2$ in RAW 264.7 Cells. To stimulate $^1O_2$ production, RAW 264.7 cells were treated with 100 ng mL^{-1} lipopolysaccharides (LPS, Sigma; 16 h) and 400 U mL^{-1} interferon (IFN)–γ (Sigma; 2.5 h). As a control, RAW 264.7 cells pretreated with LPS and IFN–γ were additionally incubated with 10 mM histidine for 15 min. 10 mM EJ1 stock solutions were prepared in DMSO (biotech grade, Sigma). An aliquot of the EJ1 stock solution was taken and diluted in fresh DMEM to a 5 μM concentration prior to cell treatments. RAW 264.7 cells pretreated with LPS and IFN–γ were washed with DPBS (Thermo Scientific) twice. The EJ1 solution in DMEM (2 mL) was added to the culture dish, and the cells were incubated for 15 min in a humidified incubator. Finally, the RAW 264.7 cells were treated with 10 nM phorbol 12-myristate 13-acetate (PMA, Sigma; 30 min). Photoluminescence micrographs were acquired through two emission channels, λ_{obs} = 410–499 nm (blue channel) and λ_{obs} = 507–691 nm (red channel). Ratiometric images were constructed by dividing the red channel images with the blue channel images. A Zeiss ZEN software was used for the image processing. Lambda profiles of the photoluminescence signals were recorded through 32 emission channels, and constructed using an OriginLab, OriginPro 8.0 software.

Phototreatments of Cells. HeLa, MCF7 and A549 cells were seeded to microscopic culture dish with poly-L-lysine coating one day before treatments. The cells were treated with 5 μM EJ1 for 15 min in a humidified incubator at 37 °C and 5% CO_2. After washing twice with DMEM, fresh DMEM was supplemented. Photoirradiation was performed inside the incubator using stripes of commercial blue LEDs.

MTT Assays. Assays were carried out according to the manufacturer's protocol (Promega, CellTiter 96® Non-Radioactive Cell Proliferation Assay). HeLa, A549 and MCF7 cells were seeded into 96-well plates one day prior to experiments. The cells were incubated with EJ1 or

cisplatin for 1 h (0.1–200 μM, 100 μL/well), and additionally incubated under blue LED photoirradiation or dark for 1 h. 15 μL of the MTT reagent was added to each well, and the cells were further incubated for 3 h at 37 °C. Finally, a 100 μL stop solution was delivered to the wells. After additional 1 h incubation, absorbance at 570 nm was recorded using a Versamax, microplate reader.

Visualization with Apoptosis Detection Kit. HeLa cells preincubated with EJ1 were treated with an Annexin V–FITC Apoptosis Detection Kit (Sigma) according to the manufacturer's protocols. Briefly, 5 μL of Annexin V–FITC and 10 μL of propidium iodide solutions were directly delivered to the culture medium. The cells were incubated for 30 min in a humidified incubator. Plasma membrane stains by Annexin V–FITC and nuclear stains by propidium iodide were visualized through emission channels at λ_{obs} = 498–560 nm and λ_{obs} = 568–673 nm, respectively.

Colocalization Experiments. HeLa cells were pretreated with 2 μM DRAQ5 (30 min), 100 nM LysoTracker Deep Red (Molecular Probes, 25 min), 1 μM ER–Tracker Red (BODIPY® TR Glibenclamide, Molecular Probes, 25 min), or 200 nM MitoTracker Deep Red FM (Molecular Probes, 30 min). After washing with DPBS twice, the cells were incubated with 5 μM EJ1 for 15 min. The cells were rinsed with fresh DMEM, and DMEM was supplemented to the culture dish. Fluorescence microscopic visualization was performed through the following emission channels: DRAQ5, λ_{obs} = 630–650 nm; LysoTracker Deep Red, λ_{obs} = 647–668 nm; ER–Tracker Red, λ_{obs} = 587–615 nm; MitoTracker Deep Red FM, λ_{obs} = 644–665 nm; EJ1, λ_{obs} = 410–499 nm and 507–691 nm. Acquisition and image analyses were carried out using a Zeiss ZEN software.

DFT/TD-DFT calculations. Quantum chemical calculations based on density functional theory (DFT) were carried out using a Gaussian 09 program.[4] Coumarin 314 in a methyl ester form was employed as a model structure for the reaction site in EJ1. An iminium form of the model compound was constructed based on the ESI MS results. Geometry optimization and single point calculations for the model structures were performed using the Becke's three parameter B3LYP exchange-correlation functionals[5–7] and the 6–311+G(d,p) basis set. The polarizable continuum model (CPCM), parameterized for water, was applied during the geometry optimization step. Frequency calculations were subsequently performed to assess the stability of the convergence. For TD–DFT calculations, the functionals and the basis sets used for the geometry optimization were applied to the optimized geometries. The polarizable continuum model (CPCM) with a parameter set for water was applied to account for solvation effects. Thirty lowest singlet and triplet states were calculated and analyzed. Simulation of the UV–vis absorption spectra were performed by employing a GaussSum program.[8]

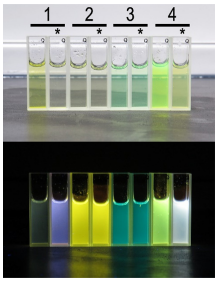

Fig. S1 Photos showing the photoluminescence changes of EJ1 (1), Irpbt–TEG (2), C314–TEG (3), and a mixture of Itpbt–TEG and C314–TEG (4) under photoirradiation in PBS buffer (pH 7.4):DMSO = 9:1, v/v: Top, under room light; bottom, under 365 nm. Cuvettes marked with asterisks are 30 min after the photoirradiation.

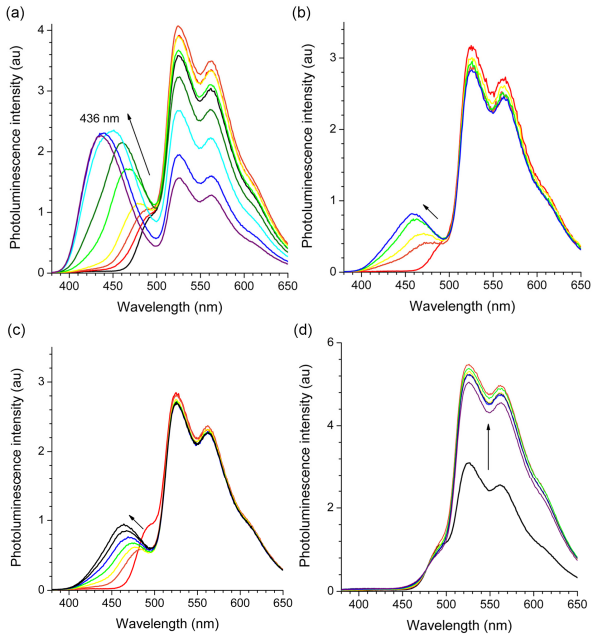

Fig. S2 Evolution of the photoluminescence spectra upon photoirradiation at 365 nm of a mixture of 10 μM Irpbt–TEG and 10 μM C314–TEG in (a) an O_2-equilibrated PBS:DMSO = 9:1 (v/v) solution and 37 °C, (b) a PBS:DMSO = 9:1 (v/v) solution containing 100 mM histidine, (c) a PBS:DMSO = 9:1 (v/v) solution containing 100 mM NaN_3, and (d) an Ar-saturated PBS:DMSO = 9:1 (v/v) solution and 37 °C.

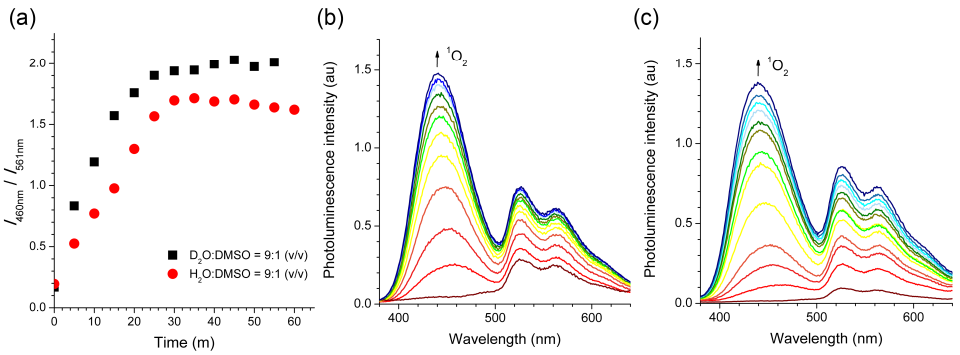

Fig. S3 Temporal evolutions of the photoluminescence intensity ratios upon 365 nm photoirradiation of EJ1 in O_2-equilibrated DMSO solutions containing either D_2O or H_2O. (a) A plot of the photoluminescence intensity ratios at 460 nm and 561 nm ($I_{460\ nm}/I_{561\ nm}$) as a function of time. (b) Spectral changes of the air-equilibrated DMSO:D_2O solution (1:9, v/v). (c) Spectral changes of the air-equilibrated DMSO:H_2O solution (1:9, v/v).

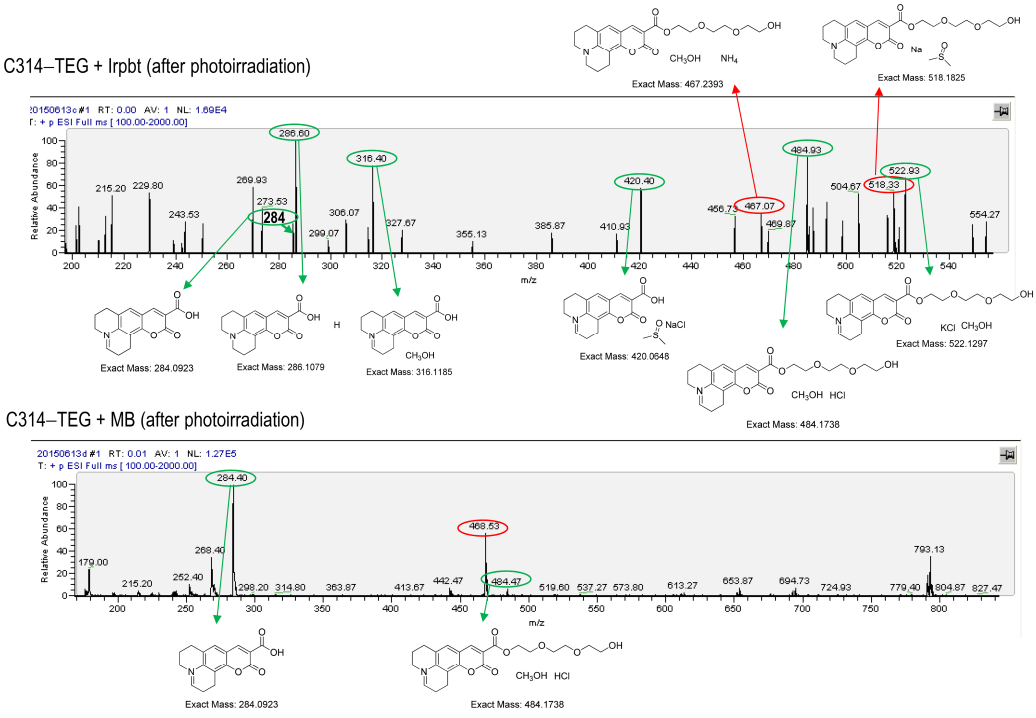

Fig. S4 ESI MS (positive) spectra for a solution containing C314–TEG and Irpbt–TEG (top) and a solution containing C314–TEG and methylene blue (bottom) after photoirradiation under 365 nm for 30 min. Chemical structures correspond to the observed peaks in the MS spectra.

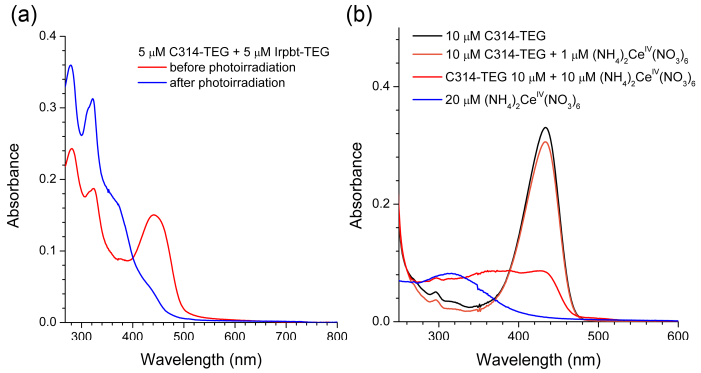

Fig. S5 (a) UV–vis absorption spectra of an aqueous buffer solution (PBS:DMSO = 9:1, v/v) containing 5 μM C314–TEG and 5 μM Irpbt–TEG before (red) and after (blue) photoirradiation (λ_{ex} = 365 nm, 30 min) at 37 °C. (b) UV–vis absorption spectra of an aqueous buffer solution (PBS:DMSO = 9:1, v/v) of 10 μM C314–TEG in the absence (black) and presence (orange and red) of $(NH_4)_2Ce^{IV}(NO_3)_6$. An absorption spectrum of 20 μM $(NH_4)_2Ce^{IV}(NO_3)_6$ (blue) is shown for comparison.

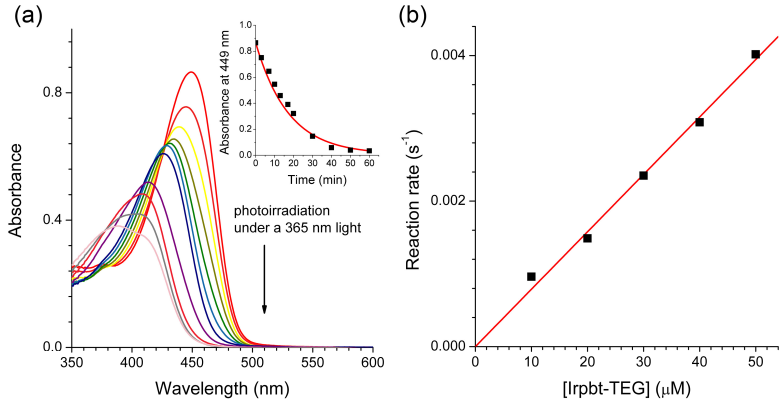

Fig. S6 (a) Temporal evolution of the UV–vis absorption spectra of an O_2-saturated aqueous buffer solution (PBS:DMSO = 9:1, v/v) containing 30 μM C314–TEG and 10 μM Irpbt–TEG upon photoirradiation (λ_{ex} = 365 nm) at 37 °C. Inset graph depicts the corresponding decrease in absorbance at 449 nm. (b) Determination of the rate constant for the $^1O_2$-mediated bimolecular reaction.

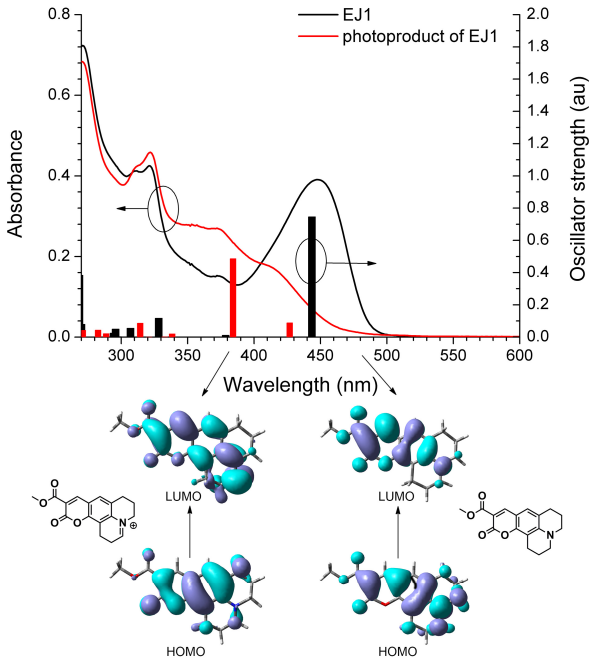

Fig. S7 Comparison of the experimental UV–vis absorption spectra (lines) and the TD–DFT calculation results (bars): Lines, UV–vis absorption spectra of 10 μM EJ1 (black line) and the photoirradiated solution of 10 μM EJ1 (red line) in PBS:DMSO = 9:1 (v/v); bars, simulated oscillator strength for the truncated form of coumarin 314 (black bars) and the iminium form of the truncated form of coumarin 314 (red bars). Inset figures show isodensity surface plots for the MOs that participate in the lowest singlet transition. Refer to the DFT/TD–DFT Calculations in the Experimental Details for the calculation procedure. Listed below are the summary of the TD–DFT calculation results:

Coumarin 314

state	energy (nm)	participating MO (expansion coefficient)	oscillator strength (au)
T_1	630	HOMO → LUMO (0.70)	-
S_1	444	HOMO → LUMO (0.80)	0.7465

The iminium form of coumarin 314

state	energy (nm)	participating MO (expansion coefficient)	oscillator strength (au)
T_1	551	HOMO–1 → LUMO (0.50) HOMO → LUMO (0.45)	-
S_1	427	HOMO → LUMO (0.67)	0.0885

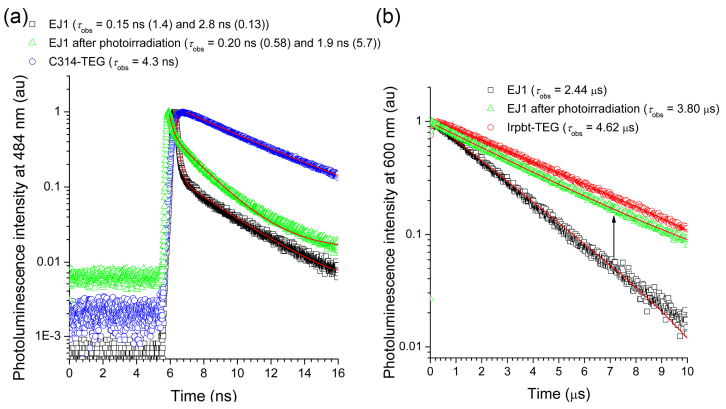

Fig. S8 Photoluminescence decay traces of 50 μM C314–TEG, 50 μM Irpbt–TEG, and 50 μM EJ1 before and after the reaction with $^1O_2$. Observation wavelengths: (a) 484 nm (coumarin 314 fluorescence) and (b) 600 nm (Irpbt phosphorescence). Decay traces were obtained after picosecond (temporal resolution = 8 ps) or nanosecond (temporal resolution = 8 ns) pulsed excitation. The traces were fitted to a monoexponential (the C314–TEG trace at 484 nm and all the traces observed at 600 nm) and a biexponential (the traces of EJ1 and the photoproduct of EJ1 observed at 484 nm) decay functions. Time constants and preexponential factor values are summarized in the figures.

The fluorescence lifetime of C314–TEG was 4.3 ns. The lifetime decreased significantly to a weighted-average lifetime (τ_{avg}) of 1.8 ns. τ_{avg} was calculated using the equation, $\tau_{avg} = \Sigma(a_i\tau_i^2)/\Sigma(a_i\tau_i)$ (i = 1 and 2), where a_i and τ_i are the preexponential factor and the time constant, respectively. The decrease in the fluorescence lifetime is indicative of energy transfer from the coumarin moiety to the Ir complex. The energy transfer rate was calculated to be 3.1×10^9 s^{-1}, using the lifetime values. The τ_{avg} value increased to 1.9 ns upon the reaction with $^1O_2$. Corresponding rate for energy transfer from the oxidized form of coumarin to the Ir complex was 3.0×10^9 s^{-1}.

The phosphorescence lifetime of Irpbt–TEG was as long as 4.62 μs. Incorporation of the Ir complex moiety into EJ1 led to a decrease in the lifetime to 2.44 μs. This decrease was most likely due to triplet–triplet energy transfer from Irpbt to the triplet state of the coumarin 314 moiety in EJ1. The decrease in the phosphorescence lifetime corresponded to a rate for the triplet–triplet energy transfer, 2.0×10^5 s^{-1}. The $^1O_2$ reaction of EJ1 restored the phosphorescence lifetime to 3.80 μs, implying that the $^1O_2$ reaction product of the coumarin 314 moiety (i.e., iminium form) has triplet state energy greater than that of Irpbt. Actually, the TD–DFT calculation results were consistent with this hypothesis (Fig. S7).

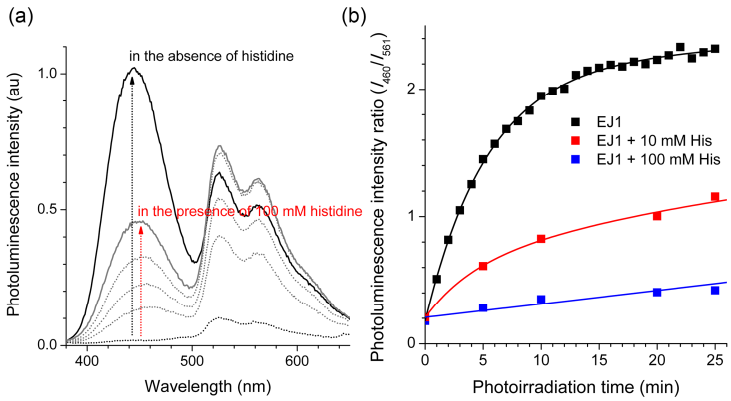

Fig. S9 (a) Evolution of the photoluminescence spectra of 10 μM EJ1 upon photoirradiation at 365 nm (30 min) in the absence (black) and presence (grey) of a $^1O_2$ scavenger, 100 mM histidine. (b) Temporal evolution of the ratios of the photoluminescence intensities at 460 nm and 561 nm of EJ1 in the absence and presence of 10 mM and 100 mM histidine. PBS:DMSO = 9:1 (v/v) and 37 °C.

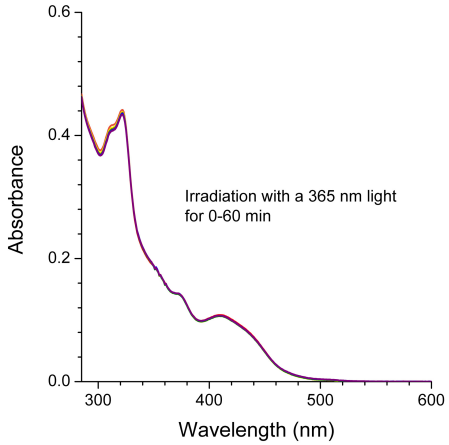

Fig. S10 UV–vis absorption spectra of 10 μM Irpbt–TEG in PBS:DMSO = 9:1 (v/v) during 365 nm photoirradiation for 60 min.

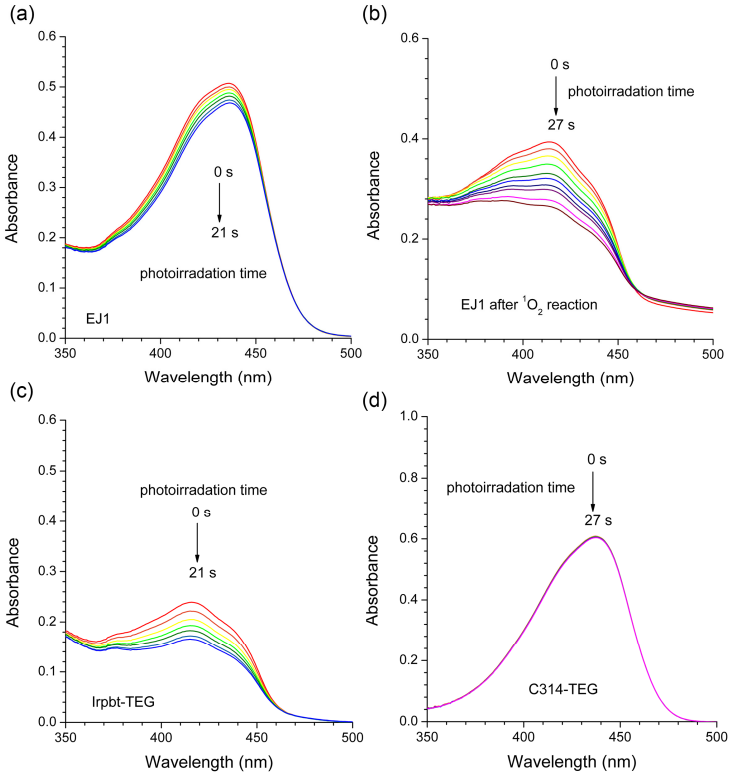

Fig. S11 Determination of $^1O_2$ photosensitization quantum yields (Φ_Δ) of (a) EJ1, (b) photoirradiated EJ1, (c) Irpbt–TEG, and (d) C314–TEG, using the methylene blue standard (Φ_Δ(ref) = 0.52). DMSO solutions containing the compound and 1,3-diphenylisobenzofuran (DPBF) as a $^1O_2$ oxidation substrate were irradiated under UV light (365 nm). Changes were monitored in the 418 nm absorption band (ΔAbs(418 nm)) of DPBF as a function of irradiation time. Φ_Δ values were calculated by the equation S1, in which *m* is the slope of a linear fit to the ΔAbs(418 nm) data and *F* = $1-10^{-\text{O.D.}}$, where O.D. refers to the optical density of the compound at 365 nm.

$$\Phi_\Delta = \Phi_\Delta(\text{ref}) \times \frac{m \cdot F_{\text{ref}}}{m_{\text{ref}} \cdot F} \qquad \text{(S1)}$$

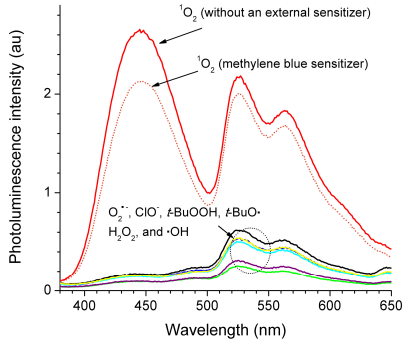

Fig. S12 Photoluminescence responses of 10 μM EJ1 to various reactive oxygen species ($^1O_2$, photosensitization by EJ1 or methylene blue; $O_2^{\bullet-}$, 1.0 mM KO_2; ClO^-, 1.0 mM NaOCl; 1.0 mM *t*-BuOOH; 1.0 mM H_2O_2; *t*-BuO•, 1.0 mM $FeSO_4$ + 100 μM *t*-BuOOH; •OH, 1.0 mM $FeSO_4$ + 100 μM H_2O_2). Refer to the Materials and General Methods for the preparation of the reactive oxygen species.

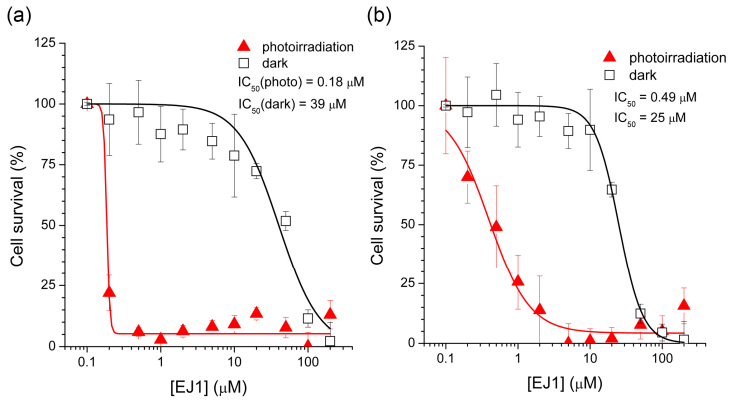

Fig. S13 MTT cell viability assays for (a) A549 and (b) MCF7. Cells pretreated with EJ1 (1 h, 37 °C) were incubated for 1 h under dark (black) and blue LEDs photoirradiation (red).

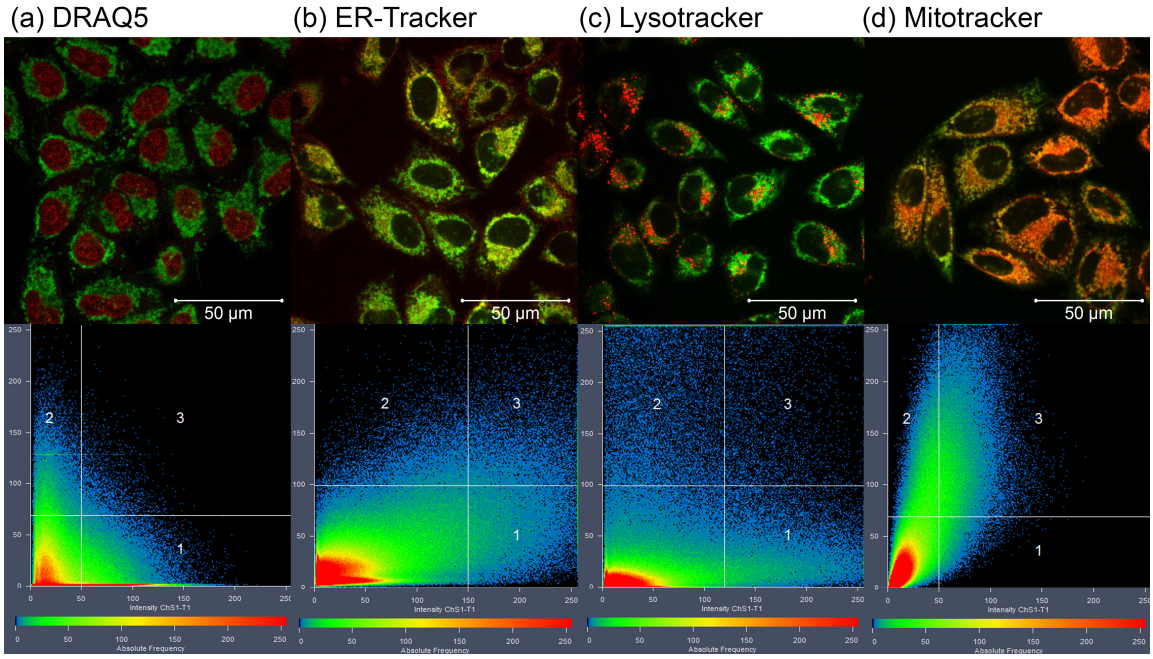

Fig. S14 Colocalization of EJ1 with organelle-specific stains. (a) DRAQ5 (nuclear stain), (b) ER–Tracker Red (ER stain), (c) LysoTracker Deep Red (lysosome stain), and (d) MitoTracker Deep Red FM (mitochondrion stain). Top panels: Overlays of the photoluminescence micrographs of EJ1 (green) and organelle-specific stains (red); Lower panels: Corresponding colocalization scatter plots. Refer to Colocalization Experiments for the conditions for cell treatments and image processing.

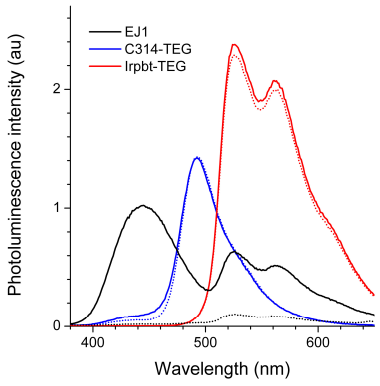

Fig. S15 Comparisons of the photoluminescence spectra of 10 μM EJ1 (black), 10 μM C314–TEG (blue) and 10 μM Irpbt–TEG (red) in PBS buffer:DMSO = 9:1 (v/v) at 37 °C before (dotted lines) and after (solid lines) the photoirradiation for 1 h.

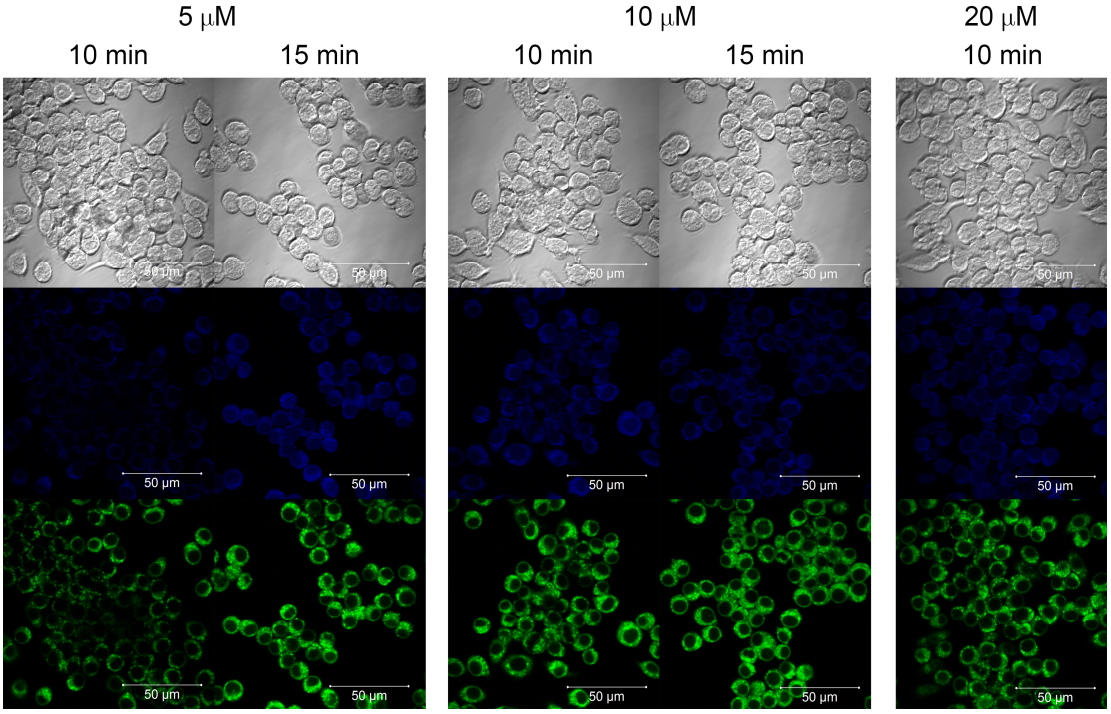

Fig. S16 Micrographs showing uptake of EJ1 by RAW 264.7 cells treated at various incubation times and concentrations: Top images, bright field images; middle images, λ_{obs} = 410–499 nm; bottom images, λ_{obs} = 507–691 nm. Scale bar = 50 μm. Note that the RAW 264.7 cells were not stimulated by LPS, IFN–γ and PMA.

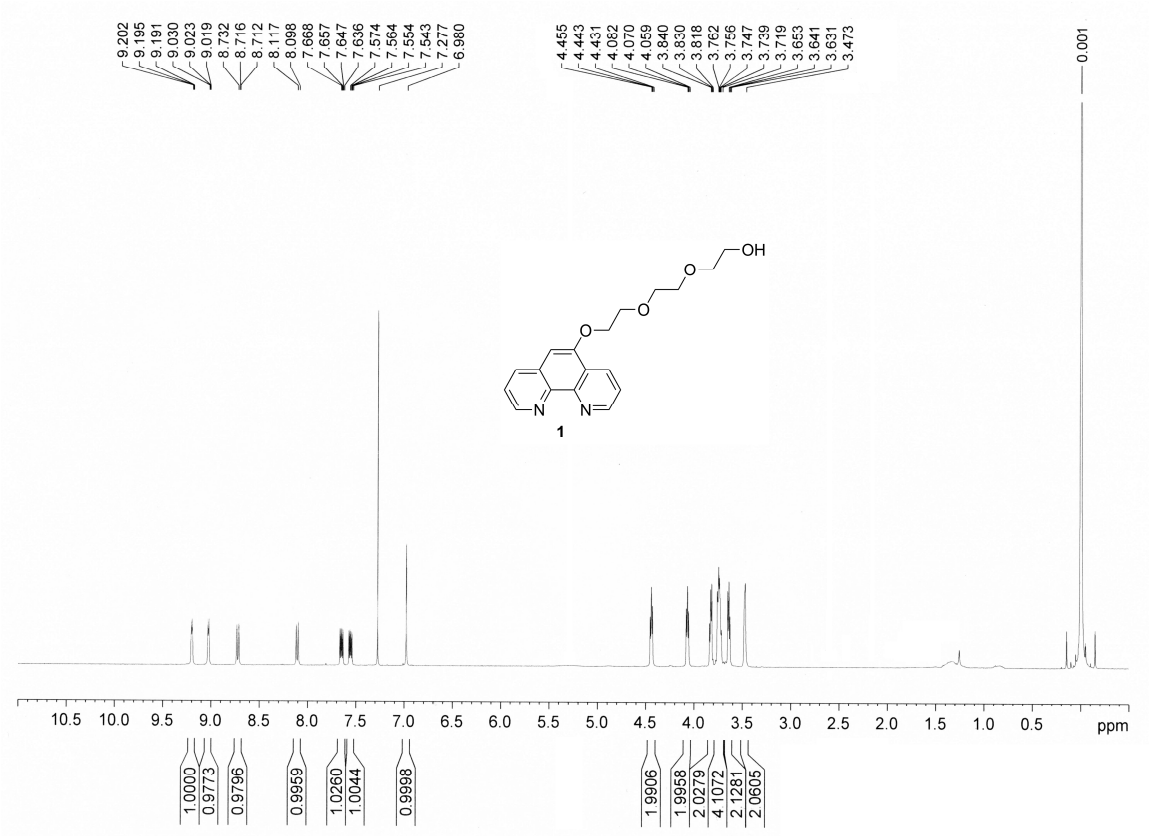

Fig. S17 ^{1}H NMR (400 MHz, $CDCl_3$) of compound **1**.

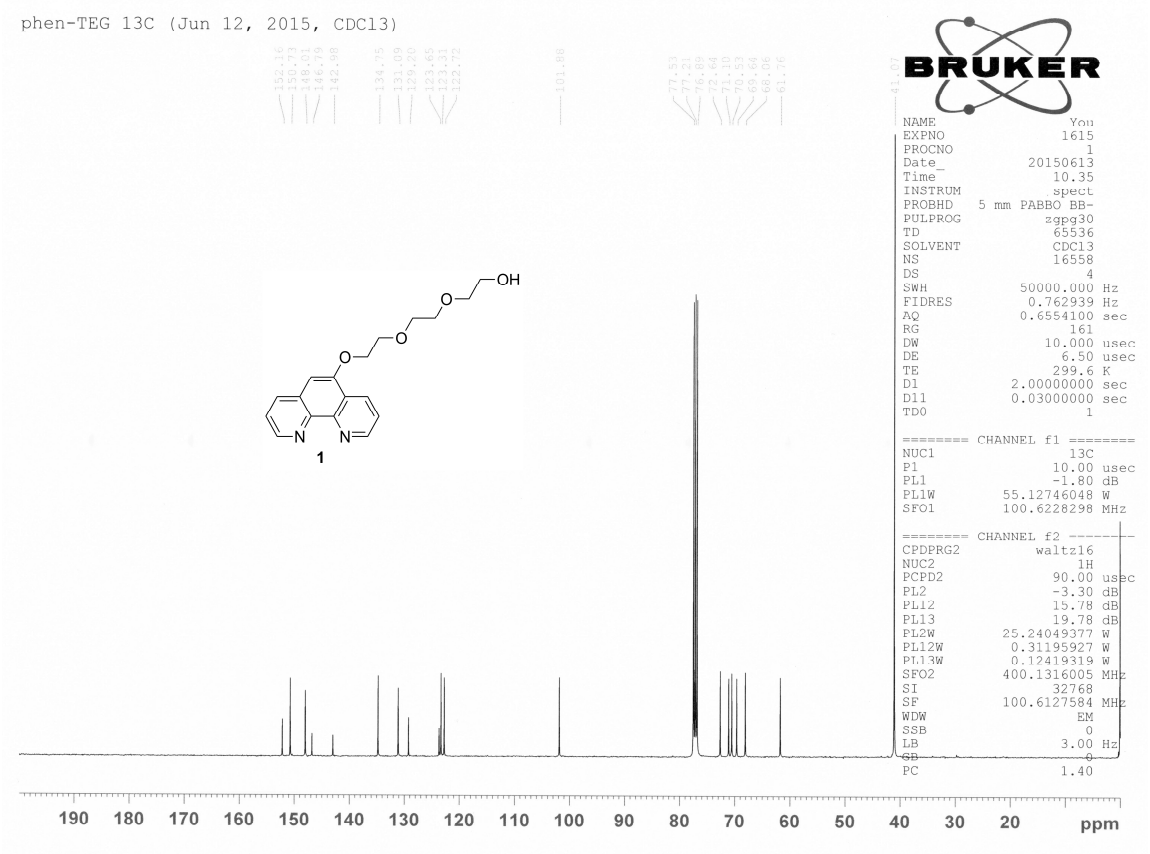

Fig. S18 $^{13}C\{^{1}H\}$ NMR (100 MHz, $CDCl_3$) of compound **1**.

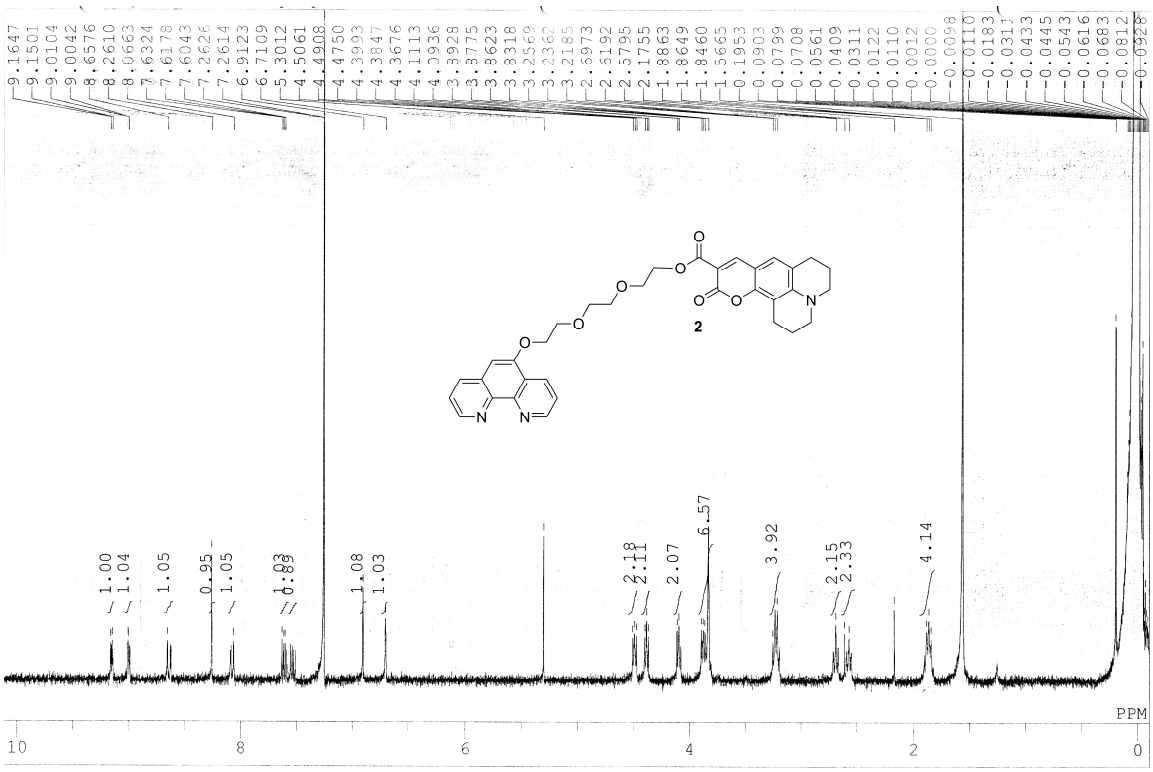

Fig. S19 ^{1}H NMR (300 MHz, $CDCl_3$) of compound **2**.

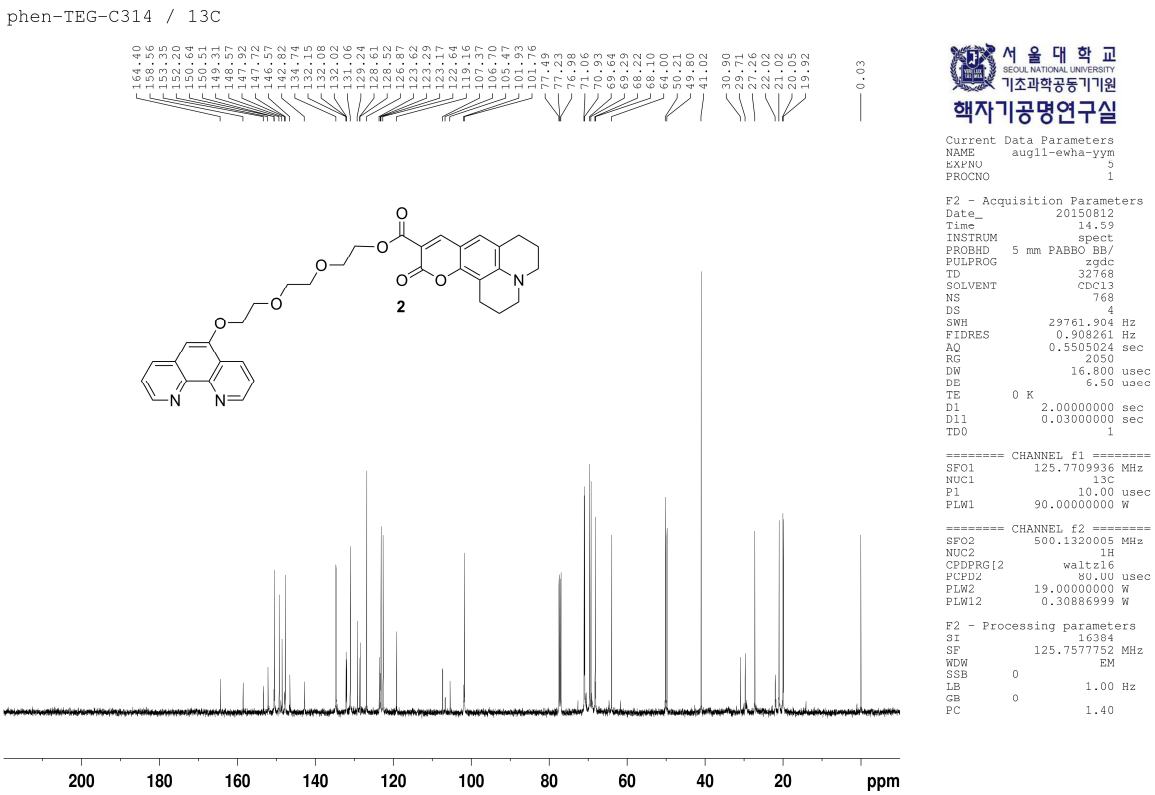

Fig. S20 $^{13}C\{^{1}H\}$ NMR (125 MHz, $CDCl_3$) of compound **2**.

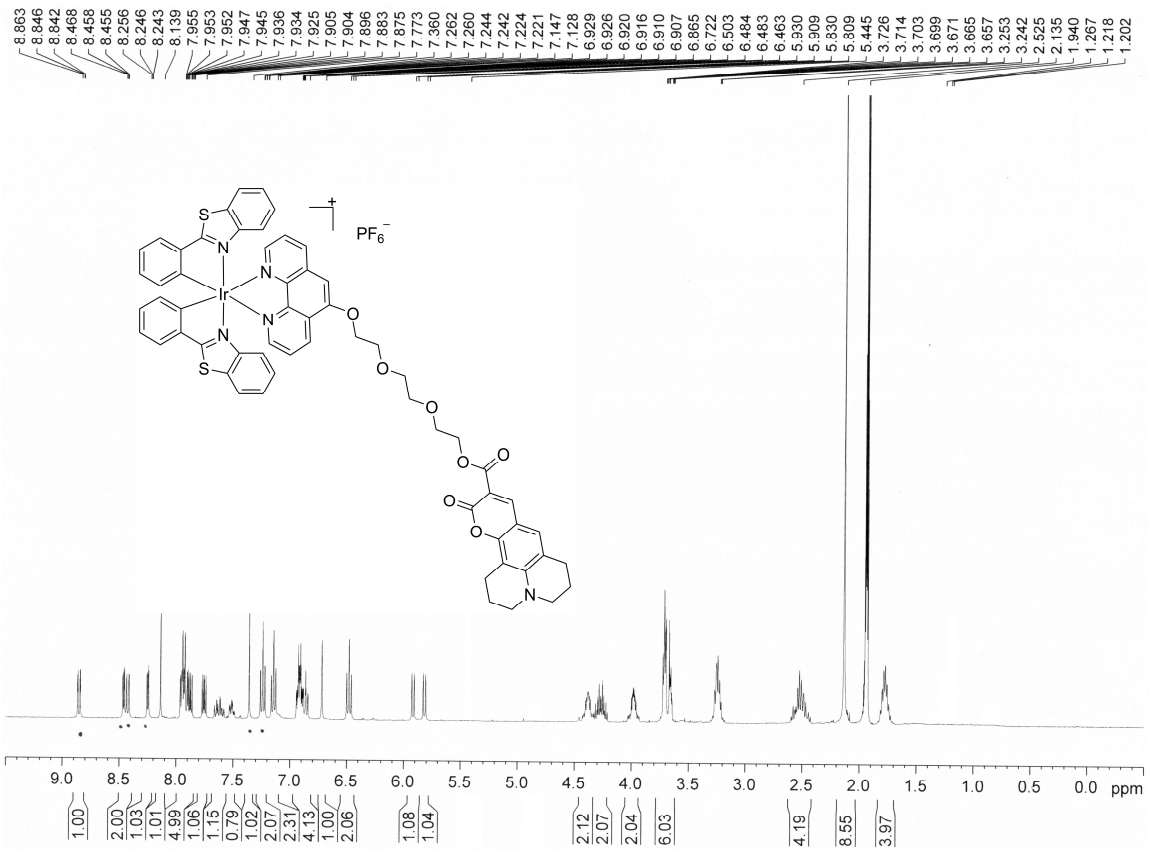

Fig. S21 ^{1}H NMR (400 MHz, CD_3CN) of **EJ1**.

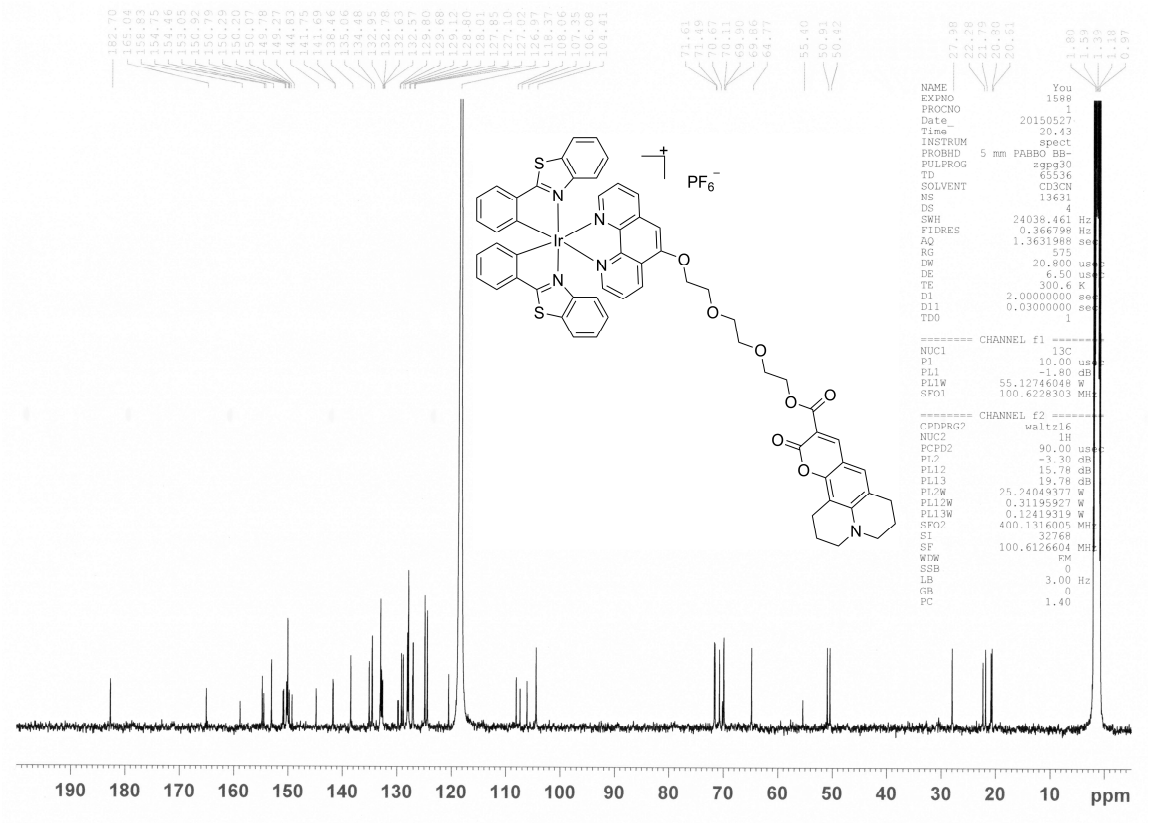

Fig. S22 $^{13}C\{^{1}H\}$ NMR (100 MHz, CD_3CN) of **EJ1**.

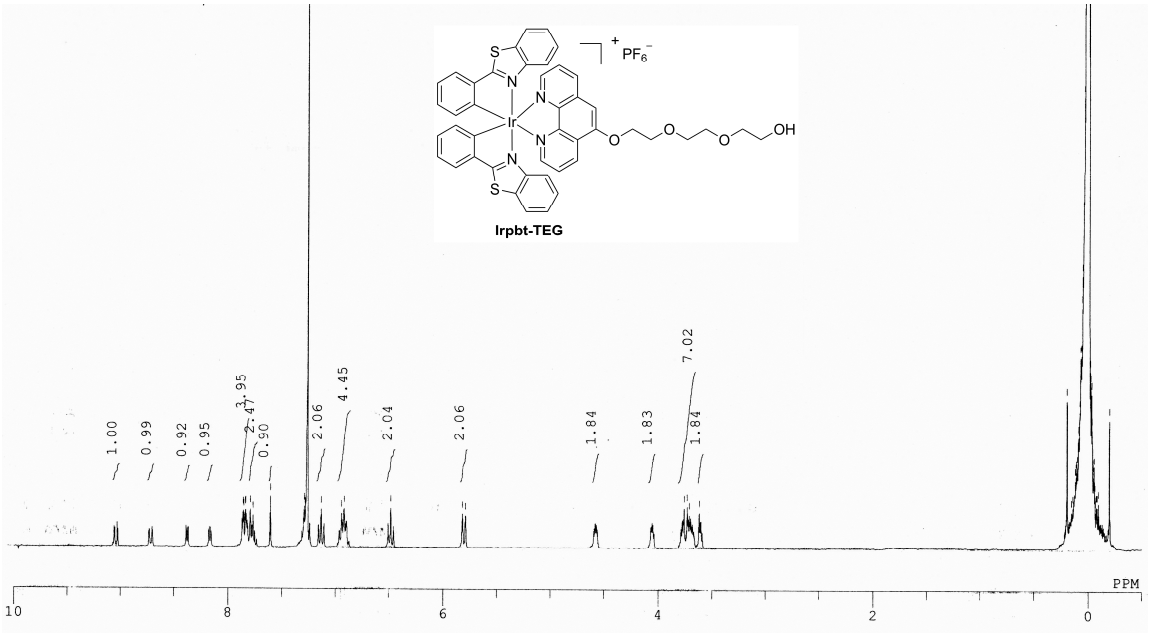

Fig. S23 ^{1}H NMR (300 MHz, $CDCl_3$) of **Irpbt–TEG**.

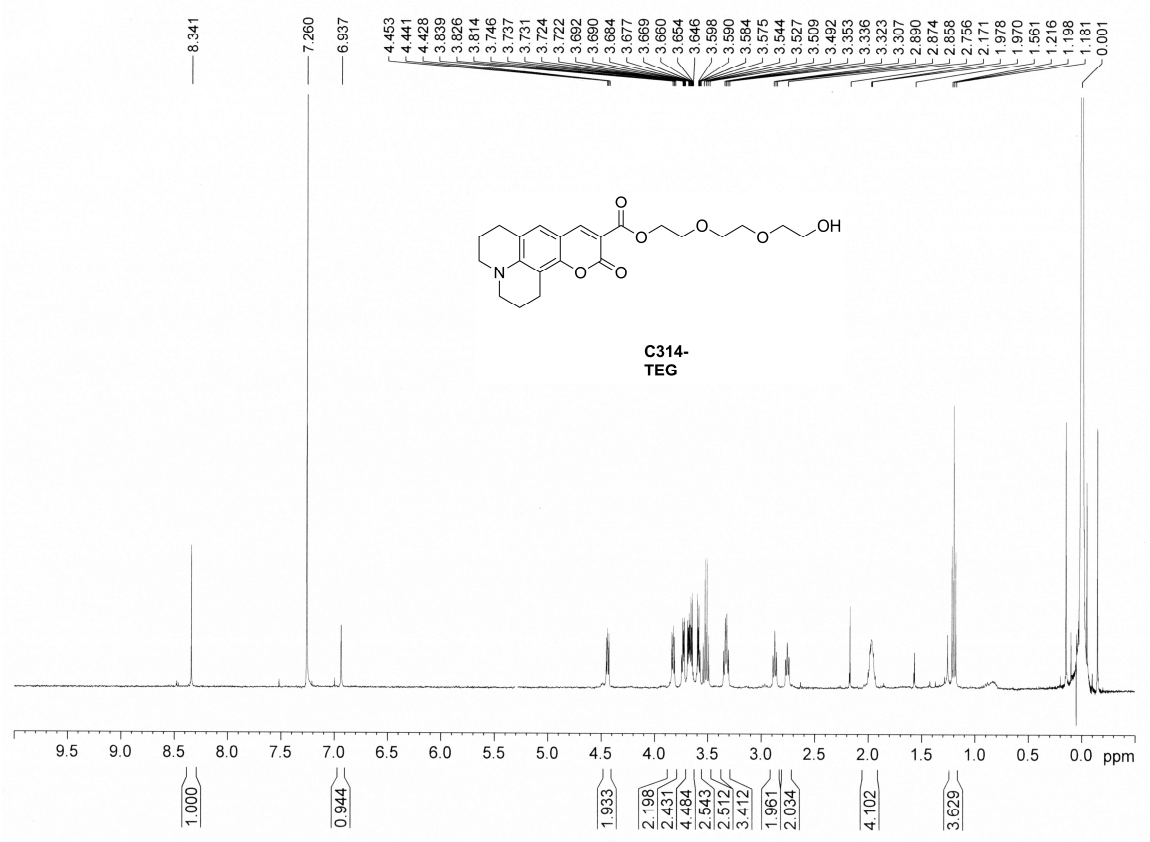

Fig. S24 ^{1}H NMR (400 MHz, $CDCl_3$) of **C314–TEG**.

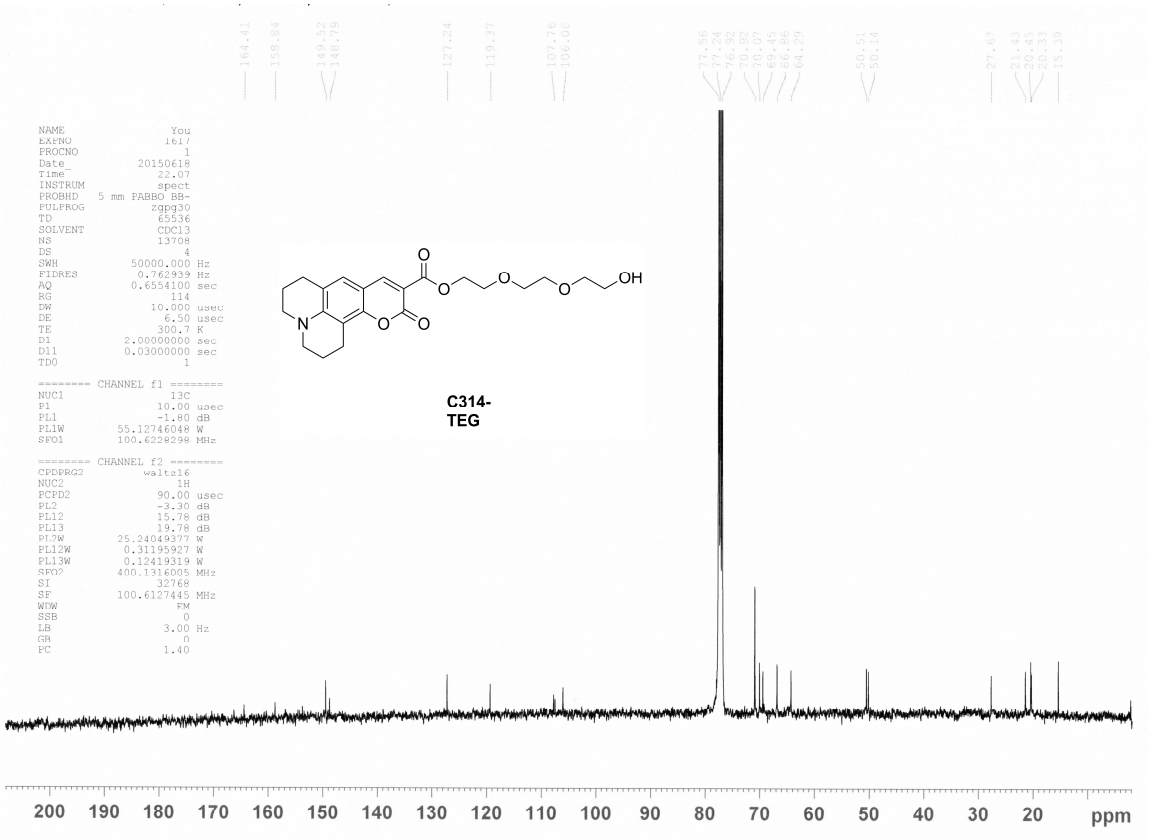

Fig. S25 $^{13}C\{^{1}H\}$ NMR (100 MHz, $CDCl_3$) of **C314–TEG**.

References

1. E. W. Miller, A. E. Albers, A. Pralle, E. Y. Isacoff, C. J. Chang, *J. Am. Chem. Soc*. **2005**, *127*, 16652.
2. Y. Chen, W. Guo, Z. Ye, G. Wang, J. Yuan, *Chem. Commun*. **2011**, *47*, 6266.
3. H. Woo, S. Cho, Y. Han, W.-S. Chae, Y. You, W. Nam, *J. Am. Chem. Soc*. **2013**, *135*, 4771.
4. M. J. Frisch, G. W. Trucks, H. B. Schlegel, G. E. Scuseria, Robb, M. A.; J. R. Cheeseman, G. Scalmani, V. Barone, B. Mennucci, G. A. Petersson, H. Nakatsuji, M. Caricato, X. Li, H. P. Hratchian, A. F. Izmaylov, J. Bloino, G. Zheng, J. L. Sonnenberg, M. Hada, M. Ehara, K. Toyota, R. Fukuda, J. Hasegawa, M. Ishida, T. Nakajima, Y. Honda, O. Kitao, H. Nakai, T. Vreven, J. A. Montgomery, Jr., J. E. Peralta, F. Ogliaro, M. Bearpark, J. J. Heyd, E. Brothers, K. N. Kudin, V. N. Staroverov, R. Kobayashi, J. Normand, K. Raghavachari, A. Rendell, J. C. Burant, S. S. Iyengar, J. Tomasi, M. Cossi, N. Rega, J. M. Millam, M. Klene, J. E. Knox, J. B. Cross, V. Bakken, C. Adamo, J. Jaramillo, R. Gomperts, R. E. Stratmann, O. Yazyev, A. J.

Austin, R. Cammi, C. Pomelli, J. W. Ochterski, R. L. Martin, K. Morokuma, V. G. Zakrzewski, G. A. Voth, P. Salvador, J. J. Dannenberg, S. Dapprich, A. D. Daniels, O. Farkas, J. B. Foresman, J. V. Ortiz, J. Cioslowski, D. J. Fox, Gaussian, Inc., Wallingford CT, 2009.

5. A. D. Becke, *J. Chem. Phys.* **1988**, *88*, 2547.
6. A. D. Becke, *J. Chem. Phys.* **1993**, *98*, 5648.
7. A. D. Becke, *Phys. Rev. A* **1988**, *38*, 3098.
8. N. M. O'Boyle, A. L. Tenderholt, K. M. Langner, *J. Comp. Chem.* **2008**, *29*, 839.